



flow of fluid through the bed and the spherical shape of the bed particles, the minimum fluidization velocity may be expressed as follows (3):

$$u_{mf} = \frac{d^2(\rho_s - \rho_f)g}{200\eta_f\phi^2} \left( \frac{\varepsilon^3}{1 - \varepsilon} \right) \quad (1)$$

where:  $d$  – diameter of the solid particle, m;  $\rho_s$  – pellets/minitables density,  $\text{kg}\cdot\text{m}^{-3}$ ;  $\rho_f$  – fluid density,  $\text{kg}\cdot\text{m}^{-3}$ ;  $\varepsilon$  – bed porosity;  $g$  – acceleration due to the gravity,  $\text{m}\cdot\text{s}^{-2}$ ;  $\eta_f$  – fluid dynamic viscosity,  $\text{Pa}\cdot\text{s}$ ;  $\phi$  – shape factor.

During the fluidization process, solid particles become suspended in a gas or liquid flow stream, circulate intensively around their axis and displace in the fluidized bed. It enables excellent interfacial fluid contact of the particles surface and the gas/liquid stream as well as very good mixing in the system (4). Fluidization as the unit operation is often applied in various technological processes of chemical industry e.q. gas-liquid or gas-solid reactions, combustion of fine coal in power plants, etc. (1, 2). Fluidization process is also often used in the food industry, where a drying step (flour, milk or coffee) is carried out (5). The pharmaceutical industry has been applying the fluidization process since the 1960s, mainly for the production of solid dosage forms, as well as during operations such as drying, mixing, granulating and coating (6).

The coating process of solid particles (pellets, granules, tablets) is applied when the active pharmaceutical ingredient (API) in the core needs to be protected from the environmental exposure (e.q. moisture, oxygen) as well as for taste masking or when the release of API should be modified for prolonged-release or gastro-resistance (7, 8). Fluid bed coating is one of the most convenient methods for

covering by polymeric film small solid cores like pellets (diameter of  $0.5 \div 2.0$  mm), granules ( $1.6 \div 3.2$  mm) and minitables ( $1 \div 3$  mm) (6).

The coating is generally performed using aqueous or organic solutions/dispersions of pharmaceutically acceptable polymers. The most common are cellulose derivatives and methacrylates both used for taste masking or modification of drug release rate (9). Film thickness, its uniformity and consequently the quality of the medicinal product depends on the method used for coating as well as on the process parameters.

In contrast to the pan coating, the fluid bed coating process may be used to coat units smaller than conventional tablets. Additionally, comparing with the pan coating, fluid bed equipment uses higher airflows, which enables faster solvent evaporation (9). A typical fluid bed apparatus consists of a perforated air distributor at the bottom of the chamber and a vertically installed nozzle (on the upper or lower side) providing the coating mixture (8).

The unique construction of the fluid bed apparatus is represented by Aircoater (Romaco Innojet, Steinen, Germany) designed by Herbert Huttlin for drying, granulation or coating processes (Fig. 1). The equipment is dedicated to run processes for cores of different sizes, starting from powders and ending with tablets. The air distributor (Orbiter) consists of overlapping circular plates with slots between them, through which air passes into the cylindrical chamber. Special design of the distributor provides low, orbital air movement. A rotating nozzle (Rotojet) is placed centrally in the distributor and sprays a coating mixture in an unusual, horizontal direction (10).

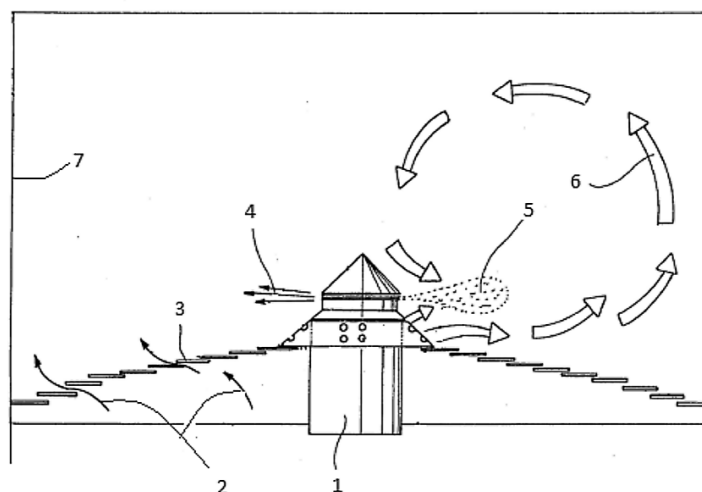


Figure 1. Fluid bed coater scheme (Aircoater 025). 1 – rotating nozzle (Rotojet), 2 – airflow, 3 – air distributor (Orbiter), 4 – spraying air, 5 – spraying of coating mixture, 6 – particles movement, 7 – chamber wall (10).

Table 1. An orthogonal array based on the Taguchi method.

Orthogonal array	No of experiments	No of factors	Max. No of factors at these levels			
			Level 2	Level 3	Level 4	Level 5
L4	4	3	3	-	-	-
L8	8	7	7	-	-	-
L9	9	4	-	4	-	-
L12	12	11	11	-	-	-
L16	16	15	15	-	-	-
L16	16	5	-	-	5	-
L18	18	8	1	7	-	-
L25	25	6	-	-	-	6
L27	27	13	-	13	-	-
L32	32	31	31	-	-	-
L32	32	10	1	-	9	-
L36	36	23	11	12	-	-
L36	36	16	3	13	-	-
L50	50	12	1	-	-	11
L54	54	26	1	25	-	-
L64	64	63	63	-	-	-
L64	64	21	-	-	21	-
L81	81	40	-	40	-	-

During the fluid-bed coating, several process parameters have to be considered with an emphasis on inlet air velocity, inlet air temperature, flow rate of the coating mixture and used spray pressure. The inlet air velocity is responsible for maintaining the proper fluidized state of the particles and their intensive mixing, which is critical for uniform coating and fast drying. Moreover, the fluidized bed expands during the coating process to accommodate the enlarged solid volume fraction, thus preventing the problem of clogging (11). To avoid bed collapse during the process, the minimum fluidization velocity should be determined and assured. However, this is not the only condition for obtaining a high-quality product.

Optimization of process parameters should involve a better understanding of the complex dynamics, however, the experimental approach is troublesome. Selection of the best parameters may be difficult and requires a number of trials. However, Design of Experiment (DoE) may be used for simplification purpose. One of the most popular DoE models used for process optimization is the Taguchi method, according to which each process may be affected by many factors, classified into two categories: signal and noise factors (12). Signal fac-

tors (S) are controllable, while noise factors (N) may be difficult to manage. According to the Taguchi method, removing noise factors is expensive and time-consuming, so the goal is to identify and select the best combination of signal factors, which leads to a high-quality product. Mathematically, it is expressed as the ratio of S to N (S/N). In this method, all examined factors are simultaneously changed (as planned on orthogonal tables) and depending on the number of parameters, the number of necessary experiments to be performed is determined (Table 1). The results of conducted experiments are compiled based on a mathematical model used for interpretation, prediction and optimization. In this way, the input variables and their actual effect on the process can be verified. Taguchi has described approximately 70 S/N interpretations, but most often three of them are used: "the larger the better", "the smaller the better" and "nominal the best" (13).

The aim of the presented study is to compare the coating of pellets (0.7-0.8 mm) and minitables (2.5 mm) in a fluid bed system and to optimize this process using the calculated minimum fluidization velocity and Taguchi method of DoE.



## EXPERIMENTAL

### Materials

Following materials were used in the study: microcrystalline cellulose (Vivapur 101 and Vivapur 102, JRS Pharma, Rosenberg, Germany), sodium stearyl fumarate (PRUV, JRS Pharma, Rosenberg, Germany), lactose (Tabletose 80 and Flowlac 100, Meggle Pharma, Wasserburg, Germany), colloidal silicon dioxide (Aerosil 200, Evonik Industries AG, Darmstadt, Germany), hypromellose (Pharmacoat 606, Harke Pharma, Mühlheim, Germany), copolymer of 2-(dimethylamino)ethyl methacrylate, butyl methacrylate and methyl methacrylate 2 : 1 : 1 (Eudragit E PO, Evonik Industries AG, Darmstadt, Germany), stearic acid (Mallinckrodt Pharmaceuticals, Hazelwood, USA), sodium lauryl sulfate (Merck, Hohenbrunn, Germany) and talc (Luzenac VAL Chisone, Porte, Italy)

### Minitablets and pellets preparation

Placebo biconvex minitables with a diameter of 2.5 mm (MT2.5) and 2.0 mm (MT2.0) were prepared by direct compression of powders using a rotary tablet press (Erweka RTP-D8, Frankfurt, Germany or Pressima MX Eu-B/D, IMA Kilian, Cologne, Germany) equipped with a single or multiple punches (13-tips).

Powder mass consisted of: spray-dried lactose (74.07%), microcrystalline cellulose (24.68 %), silicon dioxide (0.25%) and sodium stearyl fumarate (1.0%).

Placebo pellets with a diameter of 1.0-1.25 mm (P1.0) containing lactose and microcrystalline cellulose (ratio 1 : 1) were produced by extrusion and spheronization method (Extruder 025 and spheronizer, Caleva, Dorset, UK) using 5% (w/w) hypromellose solution as a binder (50 g/100 g of powders). Pellets were dried at 60°C until reaching 5% humidity. Pellet size was standardized by sieving and the 1.0 – 1.25 mm fraction was selected.

Cellulose placebo pellets with a diameter of 0.7 – 0.8 mm (P0.7) were received from Harke Pharma (Mühlheim, Germany).

Mass uniformity, as well as dimensions, were measured for 20 units. Hardness tests of minitables and pellets (n=10) were performed using a Texture Analyzer (Stable Micro Systems, Surrey, UK) with a cylindrical probe (6 mm) lowering at a constant velocity of 0.5 mm/s until the cores were crushed. Friability tests were performed according to the procedure for tablets (Ph. Eur. 9 2.9.7).

### The minimum fluidization velocity calculation

Pellets or minitables were placed in a measuring cuvette (5 cm<sup>3</sup>) and the number of particles (N) filling the vessel was counted (the procedure was repeated three times). Next, the cuvette containing the particles was filled thoroughly with paraffin. The total volume of pellets or minitables ( $V_{PT}$ ) in the measuring cuvette was found as the difference between the volume of 5 cm<sup>3</sup> ( $V_z$ ) and the volume of paraffin ( $V_{liq}$ ) filling the interparticle space ( $V_{PT} = V_z - V_{liq}$ ). The total pellets/minitables volume was divided by the counted number of particles (N) to obtain the volume of a single particle (VP).

The particle bed porosity ( $\epsilon_0$ ) was specified (Eq. 2) as the ratio of the determined volume of paraffin ( $V_{liq}$ ) to the volume of the cuvette ( $V_z$ ).

$$\epsilon_0 = \frac{V_{liq}}{V_z} \quad (2)$$

Equivalent diameter ( $d_e$ ) of a single particle was calculated (Eq. 3) as follows:

$$d_e = \left( \frac{6V_{PT}}{\pi N} \right)^{1/3} \quad (3)$$

The equivalent diameter of a pellet P0.7 was determined in the Institute of Pharmaceutics and Biopharmaceutics Heinrich-Heine University (Düsseldorf) using Camsizer XT (Retsch Technology, Haan, Germany).

The particle sphericity was obtained by dividing the equivalent sphere area of the given particle

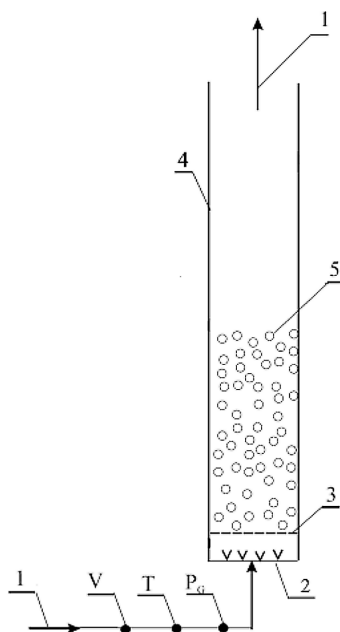


Figure 2. Experimental set-up for determination of minimum fluidization velocity (1 – air stream, 2 – fluid distributor, 3 – metal mesh, 4 – column, 5 –solid particles bed,  $P_G$ – manometer, T- thermometer, V- rotameter).

Table 2. An orthogonal array of minitabets and pellets coatings.

Batch	Inlet air temperature [°C]	Inlet air velocity [m/s]	Spray rate [g/min]	Spray pressure [bar]
MT2.5.1	37	1.3	0.6	1
MT2.5.2	37	1.2	0.5	0.8
MT2.5.3	37	1.0	0.4	0.6
MT2.5.4	34	1.3	0.5	0.6
MT2.5.5	34	1.2	0.4	1
MT2.5.6	34	1.0	0.6	0.8
MT2.5.7	31	1.3	0.4	0.8
MT2.5.8	31	1.2	0.6	0.6
MT2.5.9	31	1.0	0.5	1
P0.7.1	37	1.0	0.6	1
P0.7.2	37	0.97	0.5	0.8
P0.7.3	37	0.9	0.4	0.6
P0.7.4	34	1.0	0.5	0.6
P0.7.5	34	0.97	0.4	1
P0.7.6	34	0.9	0.6	0.8
P0.7.7	31	1.0	0.4	0.8
P0.7.8	31	0.97	0.6	0.6
P0.7.9	31	0.9	0.5	1

MT2.5.1-9 - coating trials of minitabets with a diameter 2.5 mm; P0.7.1-9 - coating trials of pellets with a diameter 0.7 mm

and the actual surface of the core (calculation based on a particle volume).

The minimum fluidization velocity ( $u_{mf}$ ) was measured using an experimental set up presented in Figure 2. At the bottom of a plexiglass column ( $D_o/D_i = 68/60$  mm,  $H = 1000$  mm), a perforated plate was installed as the air distributor. The height of the fixed core bed was 100 mm. The air (1) was introduced into the column through the teflon plate distributor (2) and then through the metal mesh (3). The airflow rate, as well as air pressure, were controlled under the gas distributor. The fluidized bed height was observed and measured. The experiments were conducted at room temperature.

The minimum fluidization porosity ( $\epsilon_{mf}$ ) was found (Eq. 4) using packed bed porosity ( $\epsilon_0$ ), packed bed height ( $H_0$ ) in the column and bed height in the column at the start of fluidization ( $H$ ):

$$\epsilon_{mf} = 1 - \frac{H_0}{H} \cdot (1 - \epsilon_0) \quad (4)$$

The pressure drop ( $\Delta P$ ) along the fluidized bed height was calculated (Eq. 5) as the difference between air pressure under the gas distributor ( $V_G$ ) and atmospheric pressure ( $P_{atm}$ ):

$$\Delta P = P_G - P_{atm} \quad (5)$$

The superficial gas velocity was calculated (Eq. 6) as follows:

$$u_G = \frac{V_G}{S} \cdot \frac{P_G}{P_{atm}} \quad (6)$$

where:

$V_G$  – volumetric gas flow rate measured using the rotameter,  $m^3 \cdot s^{-1}$

$S = \pi D_{col}^2 / 4$  – cross-section area of the column,  $m^2$

The theoretical values of the minimum fluidization velocity of minitabets and pellets were predicted using Ergun equation (Eq. 7) (2). The frictional losses for the flow through the packed bed can be expressed as the sum of viscous losses and turbulent losses represented by the Ergun equation:

$$\Delta P = \frac{150(1 - \epsilon_{mf})^2}{\epsilon_{mf}^3} \frac{\eta_F u_{mf} L_{mf}}{d_c^2} + \frac{1.75(1 - \epsilon_{mf})}{\epsilon_{mf}^3} \frac{\rho_F u_{mf}^2 L_{mf}}{d_c^2} \quad (7)$$

The product of the frictional pressure drop (Eq. 8) and the cross-sectional area of the bed must be equal to the net weight of solids in the bed expressed as:

$$\Delta P \cdot S = L_{mf} \cdot S(1 - \epsilon_{mf})(\rho_s - \rho_F)g \quad (8)$$

where:  $d_c$  – equivalent diameter of the pellets/minitabets, m;  $L_{mf}$  – height of the bed at the onset of the fluidization, m;  $\rho_s$  –

pellets/minitablets density,  $\text{kg}\cdot\text{m}^{-3}$ ;  $\rho_F$  – fluid density,  $\text{kg}\cdot\text{m}^{-3}$ ;  $\varepsilon_{mf}$  – bed porosity at the onset of the fluidization.

Combination of (Eq. 7) and (Eq. 8) results as follows (2):

$$\frac{1.75}{\varepsilon_{mf}^3} \left( \frac{d_e u_{mf} \rho_F}{\eta_F} \right) + \frac{150(1 - \varepsilon_{mf})}{\varepsilon_{mf}^3} \frac{d_e u_{mf} \rho_F}{\eta_F} = Ar \quad (9)$$

Archimedes number ( $Ar$ ) in Eq. 9 is defined as follows:

$$Ar = \frac{d_c^3 \rho_F (\rho_S - \rho_F) g}{\eta_F^2} \quad (10)$$

The minimum fluidization velocity was calculated by solving the quadratic equation obtained as a combination of (Eq. 9) and (Eq. 10).

### Coating of minitablets and pellets according to Taguchi method

The smallest (P0.7) and the largest cores (MT2.5) were coated with Eudragit E coating mixture, which is widely used as a taste masking polymer. The coating runs were performed in the bottom spray fluid bed system Aircoater 025 (Romaco Innojet, Germany). The chamber has been additionally equipped with a thermometer measuring the product temperature.

The plan of coatings was prepared according to the Design of Experiment method based on orthogonal array (Taguchi Model). The four independent variables selected to considerably affect the coating process were: inlet air temperature, air velocity, flow rate of the coating mixture and spray pressure. Each of the four parameters was considered at three levels, so according to the Taguchi orthogonal array (Table 1), it was necessary to perform 9 experiments (L9). The coating of minitablets and pellets was performed in runs according to the plan presented in Table 2.

The 50 g batches were coated to achieve a 20% weight increase. The aqueous coating mixture (15% w/w of solids) was composed of (% w/w): Eudragit E PO – 8.57, sodium lauryl sulfate – 0.86, stearic acid – 1.29 and talc – 4.28 (14). To enable the microscopic observation of the film thickness, azorubine (0.005% w/w) was added to the coating mixture as a colorant.

During experiments, the inlet air temperature, product temperature, air velocity, spraying rate, and spray pressure were controlled at 10 min intervals.

### Analysis of coated particles

To determine the film thickness, cross-sections of the coated minitablets were made using a scalpel. Cross-sections of pellets were prepared by cutting pellets (immersed in solid paraffin) with a cryotome at temperature of  $-40^\circ\text{C}$  (Shandon Cryotome E Thermo Scientific, Waltham, Massachusetts, USA). Film thickness in 10 minitablets and pellets from each batch was measured (Fig. 3) using a stereoscopic microscope (OPTA-TECH, Warsaw, Poland) equipped with OptaView software. Film thickness on minitablets was measured at 16 points, including edges, top/bottom sides and side walls. Uniformity of film thickness, as well as edge's attrition, were assessed. Additionally, the pellets were sieved through the mesh sizes of 1.0 and 1.25 mm in order to detect agglomerated particles.

In the case of minitablets, the results of the coating thickness were analyzed using Statistica 12 program (Statsoft, Krakow, Poland) with a signal to noise ratio of "nominal the best" based on the standard deviation ( $\sigma$ ) according to the Eq. 11. In the case of pellets, the results of sieve analysis were assessed based on the weight of pellets ( $Y$ ) remaining on 1.0 and 1.25 mm sieves, assuming the signal

Table 3. Characteristics of the cores.

Parameter	Pellets		Minitablets	
	P0.7	P1.0	MT2.0	MT2.5
Diameter [mm]	0.7 - 0.8	1.01 - 1.25	2.0	2.5
Height [mm]	0.7 - 0.8	1.01 - 1.25	$2.13 \pm 0.2$	$2.1 \pm 0.2$
Mass [mg]	$0.37 \pm 0.05$	$0.8 \pm 0.09$	$8.1 \pm 0.08$	$12.6 \pm 0.15$
Cores density [ $\text{kg}\cdot\text{m}^{-3}$ ]	1400	1346	1304	1340
Equivalent core diameter [mm]	0.75	1.14	2.12	2.52
Sphericity	0.87	0.87	0.86	0.80
Hardness [N]	$12.55 \pm 1.99$	$9.81 \pm 1.08$	$13.27 \pm 2.01$	$22.12 \pm 2.73$
Friability [%]	-	-	0.3	0.21

Due to the compliance of units, the SI system for diameters [m] was used in the calculations, while for the convenience of the reader the particle sizes (minitablets / pellets) were given in [mm].

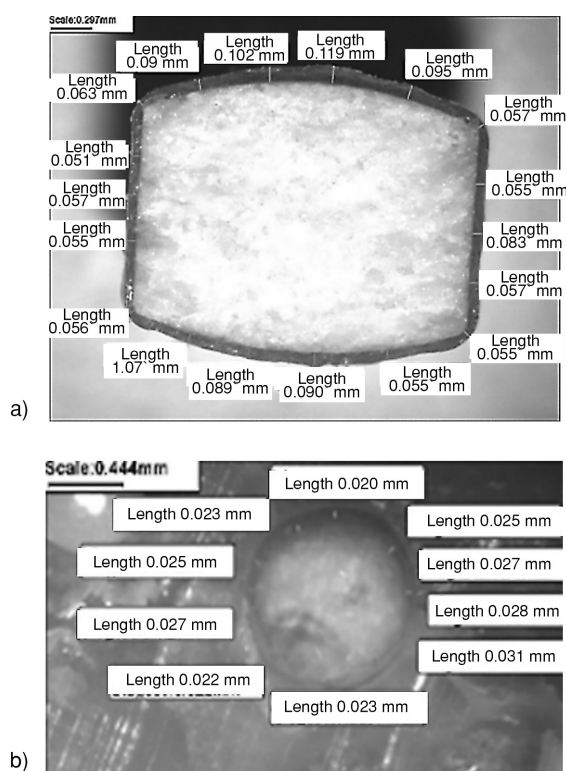


Figure 3. Cross-section area with film thickness measured on minitables (a) and pellets (b).

Table 4. Bed porosity.

Porosity	Pellets		Minitables	
	P0.7	P1.0	MT2.0	MT2.5
Fixed bed porosity	0.421	0.366	0.356	0.341
Porosity at the onset of the fluidization	0.439	0.397	0.362	0.351

to noise ratio “the smaller the better”, where  $n$  is a number of repetitions (Eq. 12).

$$S/N = -10 \cdot \log(\sigma^2) \quad (11)$$

$$S/N = -10 \cdot \log(\Sigma(Y^2)/n) \quad (12)$$

The film thickness measurements and sieve analysis results were checked by parametric tests but the normality test was unsuccessful, therefore non-parametric ANOVA (Kruskal-Wallis) analysis with Dunn’s Multiple Comparison Test was applied. P-value < 0.05 was considered as significant.

## RESULTS AND DISCUSSION

The cores of four types presented in Figure 4 were investigated. They differed both in shape and

size. Not only size but also geometry of minitables and pellets was different. Placebo minitables with a diameter of 2.0 mm (MT2.0) and 2.5 mm (MT2.5) were prepared by the direct compression method. Placebo pellets with a diameter in the range 1.0-1.25 mm (P1.0) were produced by extrusion and spherulization method. Additionally, pellets with a diameter of 0.7-0.8 mm were used as purchased from a manufacturer.

The characteristics of the cores subjected to the coating process are presented in Table 3, while in Table 4 the bed porosity determined under static and dynamic conditions is shown. The density of P1.0 and MT2.5 was similar, while P0.7 had the highest and MT2.0 the lowest density. It is noteworthy that the shape factor for P1.0 and MT2.0 is similar. P0.7

was the most spherical, while MT2.5 the least. The bed formed by P0.7 was characterized by the largest porosity (before and during  $u_{mf}$ ), while the least porous bed was formed by minitablets.

Minitablets and pellets of various dimensions were used as the solid phases in the fluidization process investigations with air as a medium. Pressure drop as a function of air flow was measured experimentally. It is well known that the bed expands as the fluid velocity increases and eventually begins to fluidize at a certain velocity ( $u_{mf}$ ), which is the hydrodynamic border between the fixed and fluidized bed. The pressure drop in the bed is almost constant if the air velocity is between the minimum fluidization velocity and the falling particles velocity (15).

Critical factors may be presented by Archimedes (Ar) and Reynolds (Re) numbers, which are dimensionless values used to describe models and real systems, such as the movement of particles in a medium (e.g. air, water). The values of Reynolds describe the ratio of inertial forces to viscosity forces during the movement of gases or liquids (Table 5) while Archimedes number represents the ratio of buoyancy forces to internal friction forces (Fig. 5).

Low values of Reynolds number indicate that minitablets and pellets fluidization in the air is more

affected by viscosity than inertia, which may be explained by their small dimensions. Reynolds number in the range of  $10 = Re = 200$  confirm that the studied cores belong to group II, according to the classification created by Saxen and Ganzh (16). Group II, based on the values of Re and Ar, can be divided into two categories:

- IIA – for  $10 \leq Re \leq 40$  and  $21\,700 \leq Ar \leq 130,000$ ,
- IIB – for  $40 \leq Re \leq 200$  and  $130\,000 \leq Ar \leq 1.6 \times 10^6$ .

The tested pellets belong to group IIA, for which the boundary air layer surrounding the particles changes from laminar to turbulent, while minitablets already belong to group IIB, which indicates rather turbulent air movement in the nearest area. Turbulent air movement in the boundary layer together with geometry of minitablets which promotes attrition may be the cause of the impeded film deposition on edges.

The values of the minimum fluidization velocity  $u_{mf}$  for minitablets and pellets were calculated from Ergun equation (Eq. 7) and compared with the experimental results (Table 6).

As expected,  $u_{mf}$  increases with an increase in the diameter of the cores. The lowest experimental  $u_{mf}$  was obtained for P0.7 (0.304 m/s), while for MT2.5 it was more than twice as large (0.625 m/s).

Table 5. Dependence  $Ar_{air} = f(Re_{air})$  at the onset of the fluidization in the air.

Cores	$Re_{air}$	$Ar_{air} = f(Re_{air})$
P0.7	17.1	$23076 = 20.7 Re_{air}^2 + 994.6 Re_{air}$
P1.0	32.9	$77888 = 27.9 Re_{air}^2 + 1445.6 Re_{air}$
MT2.0	90.5	$485280 = 36.9 Re_{air}^2 + 2019.0 Re_{air}$
MT2.5	118.1	$830000 = 40.5 Re_{air}^2 + 2253.5 Re_{air}$

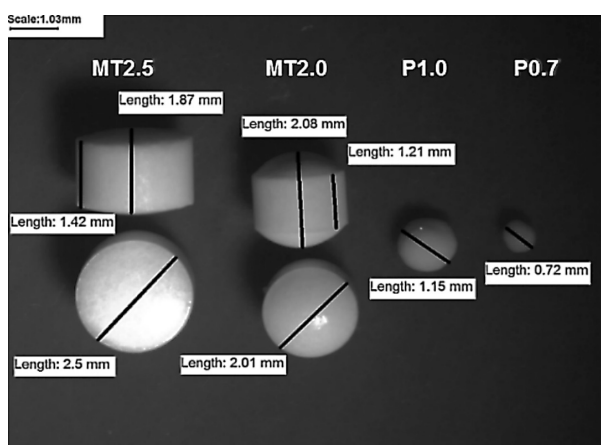


Figure 4. Axial vertical and horizontal cross-sectional view of the minitablets (MT2.0; MT2.5) and spherical pellets (P0.7; P1.0).



Table 6. Theoretical and experimental values of the minimum fluidization air velocity.

Cores	$u_{mf}^{exp}$ [m.s <sup>-1</sup> ]	$u_{mf}^{calc}$ [m.s <sup>-1</sup> ]	$\frac{u_{mf}^{calc} - u_{mf}^{exp}}{u_{mf}^{exp}} 100\%$
P0.7	0.304	0.318	4.6
P1.0	0.370	0.403	8.9
MT2.0	0.540	0.596	10.4
MT2.5	0.625	0.699	11.8

$u_{mf}^{exp}$  - experimental minimum fluidization velocity,  $u_{mf}^{calc}$  - calculated minimum fluidization velocity.

Table 7. Average film thickness on coated minitabets MT2.5 and pellets P0.7.

Batch	MT2.5						P0.7	
	Edges		Side walls		Top/bottom sides		[μm]	CV [%]
	[μm]	CV [%]	[μm]	CV [%]	[μm]	CV [%]		
1	50.0	12.8	66.0	11.6	83.0	14.1	24.0	14.1
2	57.0	13.7	68.0	11.6	87.0	17.8	26.0	10.1
3	65.0	14.9	75.0	14.0	86.0	19.0	26.0	9.0
4	64.0	13.2	69.0	6.2	89.0	17.1	26.0	8.3
5	55.0	10.5	68.0	9.0	85.0	18.7	28.0	19.1
6	48.0	16.1	64.0	13.7	77.0	20.8	26.0	9.7
7	52.0	12.4	65.0	11.0	82.0	14.7	25.0	7.8
8	67.0	15.3	67.0	17.8	86.0	26.7	24.0	12.0
9	38.0	30.5	74.0	13.7	89.0	19.2	23.0	13.0

The smallest relative difference between calculated and experimental value was obtained for P0.7 (4.6%), while the largest for MT2.5 (11.8%). The smaller relative difference obtained for MT2.0 than for MT2.5 should not be explained only by the size, but also considering the shape of MT2.0, which is more like a large pellet than a tablet. The influence of shape on fluidization has been already described. (17). Non-spherical particles have poor fluidizing properties as compared to spherical particles in terms of pressure drop or  $u_{mf}$ . Even with the same volume-equivalent diameter, non-spherical particles have lower  $u_{mf}$ . This may explain larger differences in calculated and experimental values for minitabets than for pellets.

Eighteen runs of MT2.5 and P0.7 coatings were performed according to the Taguchi model (Table 2). The inlet air temperature and spray rate were set to provide a product temperature in the range of 25-35°C which is recommended by Eudragit E PO manufacturer. In theory, the minimum fluidization velocity should be sufficient to fluidize the particles. In practice, however, this value gives only general orientation while to main-

tain the bulk of the particles in the constant movement during the process velocity of air should be kept at the value above  $u_{mf}$  (4). To ensure regular particles movement in the Aircoater, without the bed collapsing, the lowest tested inlet air velocity for minitabets was set at 50% higher than experimental  $u_{mf}$ . In the case of pellets, the assessed inlet air velocity was 200% of  $u_{mf}$  since it was additionally forced by the operating limit (minimum value at the operating scale) of the coating apparatus.

The coating process in almost all runs was conducted without problems and only during two out of 18 runs problems with the decrease in bed temperature and polymeric dust were noted.

The film thickness on the cores was measured. The average values and variation coefficient (CV) are presented in Table 7. Film thickness on minitabets differs depending on the measurement site (18). The thinnest film was observed at the edges (38-67 μm), while the thickest at the top/bottom sides (77-89 μm). Coatings were not uniform (Fig. 6), with the largest deviations (CV 30.5%) at the edges in the last batch (MT2.5.9), which differs the most from others ( $p < 0.05$ ). The most uniform

film was deposited on the MT side walls, where the smallest CV value (6.2%) was determined for batch No. 4.

The coating layer on pellets (Table 7) was uniform, characterized by the thickness in the narrow range of 23-28  $\mu\text{m}$  with CV smaller than 19.1% (lack of statistical differences between batches). Based on a poor differentiation between batches, one can assume that in the case of pellets the film thickness is not a good quality attribute for optimization of coating process parameters. Agglomerated particles are an indicator of the poor

quality coating process, hence sieve analysis was performed for coated P0.7. The results are presented in Table 8. The best results were obtained for batches No. 2, 4 and 5, where only 1% of pellets remained on the sieves. In the last two coatings almost 16% and 9% of bonded pellets were detected, respectively.

Determination of the best coating parameters for minitables and pellets, based on statistical analysis (S/N ratio) was conducted taking into consideration the coating process parameters as an input, while for output the film thickness on

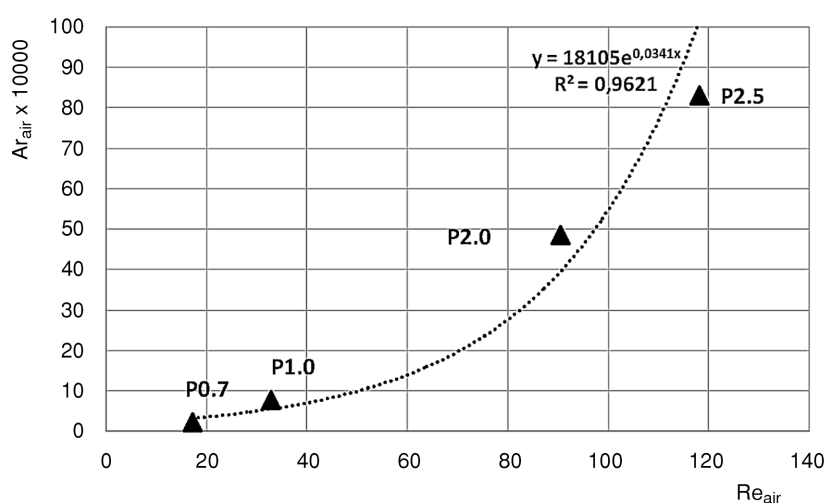


Figure 5. Dependences  $Ar = f(Re)$  at the onset of the P and MT fluidization.

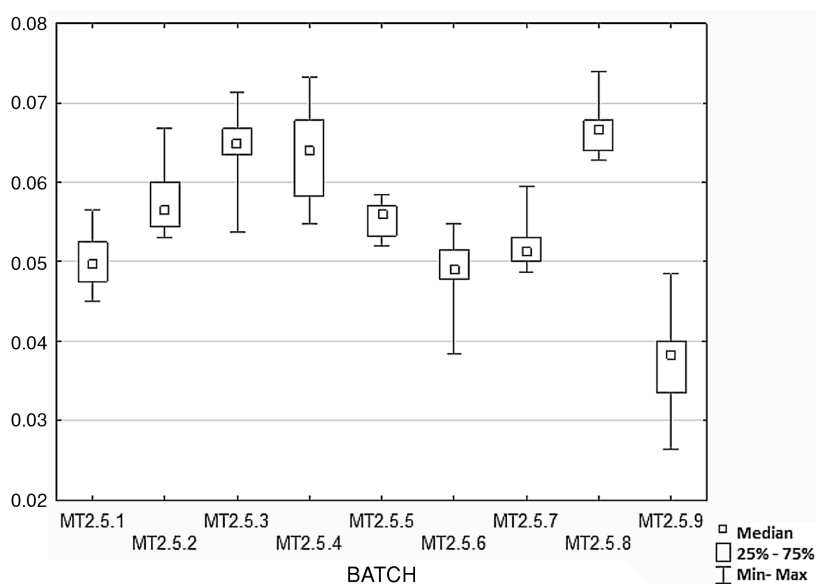


Figure 6. Film thickness on edges of minitables from nine different process conditions.

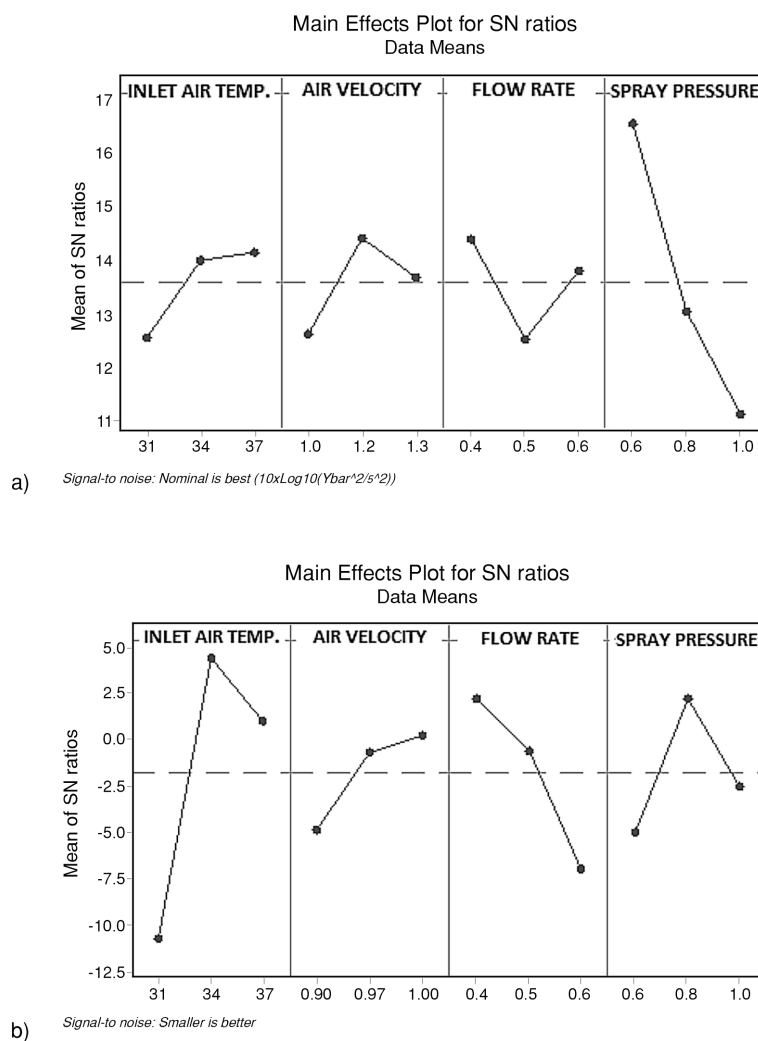


Figure 7. Plot of S/N ratio for MT2.5 (a) and P0.7 (b) coating parameters.

minitables and the amount of agglomerated pellets were chosen. In Figure 7a results from the statistical analysis of coated minitables with S/N ratio “nominal is best” are presented.

In the case of minitables, the main problem seems to be the presence of the edges that need to be covered uniformly by a polymer film what is more difficult than on flat surfaces, while at these sites the film is the most sensitive to abrasion. It was found (Fig. 7a) that the largest impact on the uniformity of film deposition has a spraying pressure ( $p < 0.05$ ), which is responsible for the polymer droplet size. A strong influence of the coating mixture flow rate on the film thickness on the top / bottom surface of MT2.5 was also demonstrated ( $p = 0.039$ ). Other investigated parameters, like inlet air temperature or air velocity, are of minor importance.

Different range of parameters was noted in the case of pellets (Fig. 7b), where sieve analysis results were assigned as an output with the assumption “the smaller the better”. To achieve the lowest level of bonded particles occurrence the inlet air temperature should be the most controllable parameter ( $p < 0.05$ ). Other important parameters include the flow rate and the spray pressure, while the air velocity was less critical.

Based on the largest values of S/N ratio, the best coating parameters for minitables and pellets were chosen (Table 9). To verify results obtained employing statistical analysis, the last two runs of coating pellets and minitables were performed using these optimal parameters.

Compared with pellets, higher inlet air temperature and velocity were chosen as optimal for minitables, while a spray pressure was lower. The

Table 8. Sieve analysis for P0.7 performed after coatings.

Batch	Pellets size [%]		
	< 1.0 mm	1.0-1.25 mm	> 1.25 mm
1	97.94	1.97	0.09
2	99.36	0.61	0.03
3	98.21	1.63	0.16
4	99.09	0.86	0.05
5	99.27	0.39	0.34
6	98.54	1.39	0.07
7	98.41	1.54	0.05
8	84.42	6.06	9.52
9	91.41	2.56	6.03

Table 9. Optimal coating parameters for MT2.5 and P0.7 based on the Taguchi method.

Batch	Inlet air temp. [°C]	Inlet air velocity [m/s]	Flow rate [g/min]	Spray pressure [bar]
P0.7	34	1.0	0.4	0.8
MT2.5	37	1.2	0.4	0.6

best inlet air velocity for minitables was twice a  $u_{mf}$  value, while for pellets it was more than triple.

During the final coating of minitables and pellets, no difficulties were observed. Both the fluid bed and the product temperature were stable. Film thickness on minitables coated according to the best selected parameters was uniform. At the edges, the film thickness was  $63 \mu\text{m}$  ( $\pm 13\%$ ), on the side walls  $70 \mu\text{m}$  ( $\pm 12\%$ ) and on the top/bottom sides  $88 \mu\text{m}$  ( $\pm 15\%$ ). In case of pellets coated under optimal conditions the film thickness was similar to that previously obtained ( $26.0 \mu\text{m} \pm 8\%$ ), however, the main difference was the decreased number of bonded particles (only 0.25% of units with a size above 1.0 mm were detected,  $p < 0.05$ ).

The bottom sprayed fluid bed systems are mainly used for coating of small particles like pellets, while tablets are coated in pan coaters. The Aircoater apparatus is a special system designed for fluid bed coating of solid particles with a broad range of sizes, from pellets up to larger tablets. While in the industry tablets are coated mostly in pan coaters, therefore, it seems appropriate to better characterize the coating process for minitables in a fluidized-bed apparatus and to compare it with the process applied to pellets. Fast selection of optimal process parameters, based on uniformity of the coating film, may be helpful not only at the early level of drug development but also during the scaling-up.

The presented research demonstrates that it is possible to achieve the best parameters of the coating

process for minitables and pellets by using the calculated  $u_{mf}$  values and Design of Experiment based on the Taguchi method. Both methods may be very useful in the industry during scaling up. Calculation of  $u_{mf}$  may be helpful during setting the inlet air ranges while the Taguchi method for choosing the optimal parameters for the coating process. Selection of parameters selection for minitables was done based on the film thickness measurements, while for pellets on the sieve analysis. The best parameters differ, depending on the size of the cores. The best inlet air velocity for minitables was double  $u_{mf}$ , while for pellets it was three times higher than  $u_{mf}$ . It can be explained by a larger total surface area in minitables, which enables faster water evaporation.

## CONCLUSIONS

Minitables and pellets have been fluidized in the air streams. According to the expectations, the fluid velocity value at the beginning of fluidization increases if the diameter of the cores increases.

Based on experiments with minimum fluidization velocity and design of experiment made by the Taguchi model, the best process parameters for coating of pellets and minitables in Aircoater apparatus were successfully selected. Experimental and theoretical outcomes were slightly in better agreement for pellets than for minitables, which may be explained by the non-spherical shape of minitables.

### Acknowledgments

Special thanks for technical support to dr Klaus Knop and dr Friederike Folltmann from the Institute of Pharmaceutics and Biopharmaceutics Heinrich-Heine-University in Düsseldorf.

The project was funded under the Applied Research Program of The National Centre for Research and Development: "Minitablets, as the new oral dosage form – the development of the preparation, coating and dosing and optimization of physical properties depending on the application" (PBS1/A7/3/2012).

### Conflict of interest

The authors declare no conflicts of interest.

### REFERENCES

1. Davidson J.F., Harrison D.: Fluidization. p. 847, Academic Press, London 1971.
2. Levenspiel O.: Engineering Flow and Heat Exchange. p. 366, Plenum Press, New York 1984.
3. Yang W.C.: Handbook of fluidization and fluid-particle systems, Marcel Dekker, New York 2003.
4. Gibilaro L.G.: Fluidization-dynamics?: The formulation and applications of a predictive theory for the fluidized state. p. 256, Butterworth-Heinemann, Oxford 2001.
5. Smith P.: Applications of Fluidization to Food Processing. p. 264, John Wiley & Sons, USA 2008.
6. Swarbrick J.: Encyclopaedia of Pharmaceutical Technology. p. 4372, Informa Healthcare 2007.
7. Pharmaceutical Manufacturing Handbook. Gad SC, editor, p. 1370, Published by John Wiley & Sons, Inc., Hoboken, New Jersey 2008.
8. Behzadi S.S., Toegel S., Viernstein H.: Recent Pat. Drug Deliv. Formul. 2, 209 (2008).
9. Felton L.A., Porter S.C.: Expert Opi. Drug Deliv. 10, 421 (2013).
10. Huttlin H.: Apparatus for treating particulate material. US 2006/0112589 A1, 2006.
11. Cahyadi C., Koh J.J.S., Loh Z.H., Chan L.W., Heng P.W.S.: AAPS PharmSciTech. 13, 1276 (2012.)
12. Dehnad K.: Quality control, robust design and the Taguchi method. p. 323, Pacific Grove: Wadsworth & Brooks/Cole Advanced Books & Software 1989.
13. Ghica M.V., Popa L., Şaramet G., Leca M., Lupuliasa D., Moiescu Ş.: Farmacia 59, 321 (2011).
14. Kluk A., Sznitowska M.: Świat Przem. Farm. 1, 22 (2012) (in Polish).
15. Passos M.L., Barrozo M.A.S., Mujumdar A.S.: Fluidization Engineering. Practice. p. 276, Laval, Kanada 2013.
16. Hartnett J.P., Irvine T.F.: Advances in Heat Transfer. p. 365, Academic Press, New York 1989.
17. Liu B., Zhang X., Wang L., Hong H.: Particuology 6, 125 (2008).
18. Czajkowska M., Sznitowska M., Kleinebudde P.: Int. J. Pharm. 495, 347 (2015).

© 2020 by Polish Pharmaceutical Society. This is an open access article under the CC BY NC license (<http://creativecommons.org/licenses/by/4.0/>).

